2.L

Nuclear Physics 39 (1962) 541—550; © *North-Holland Publishing Co., Amsterdam*

THE SCATTERING OF PROTONS FROM He^3

T. A. TOMBRELLO †, C. MILLER JONES, G. C. PHILLIPS and J. L. WEIL

Rice University, Houston, Texas ††

Received 18 June 1962

Abstract: The elastic scattering of protons from He^3 has been investigated from 2.0 to 4.8 MeV with the Rice University Van de Graaff accelerator and a small-volume, gas scattering chamber. Nine excitation curves were measured for centre-of-mass angles between 39.23° and 166°, and angular distributions have been measured for proton energies of 2.01, 3.01, 3.99, and 4.54 MeV. The phase shifts derived from these experimental data and from the data obtained at other laboratories are compared with the theoretical calculations of Bransden and Robertson. These results tend to favour the Serber rather than the symmetrical type of exchange interaction for the nucleon-nucleon potential.

1. Introduction

Recent controversy over the existence of excited states of the alpha particle has served to indicate how little is actually known about one of the simplest nuclear systems. Three states have been proposed for excitations between 20 and 30 MeV with assignment 0^+ (ref. [1]), 2^- (ref. [2]) and 1^- (ref. [3]), but none of the experimental evidence presented can be taken as conclusive proof of their existence. It is generally agreed, however, that any anomalies present are quite broad and thus correspond to very short-lived nuclear configurations.

Since it is expected that some of the proposed states have isospin, $T = 1$, it is worthwhile to investigate this energy region in Li^4 through the elastic scattering of protons from He^3. Several previous experiments have studied this reaction in this range of energies. Famularo *et al.* measured two excitation curves and four angular distributions between 1.0 and 3.5 MeV [4]); and isolated angular distributions have been measured for proton energies between 5 and 10 MeV (refs. [5-8])).

Phase shift analyses of these results have been made by Lowen [9]) and by Frank and Gammel [10]), and resonating group calculations by Bransden *et al.* have attempted to explain the data in terms of the nucleon-nucleon potential [11]).

2. Apparatus

In the present work, four angular distributions and nine excitation functions have been measured using the Rice University 5.5 MeV Van de Graaff accelerator and a

† Now at the California Institute of Technology, Pasadena, California.

†† Work supported in part by the U. S. Atomic Energy Commission.

precision small-volume, gas scattering chamber. This scattering chamber has been described recently [12]) and the present discussion will be confined to details pertaining to the present experiment. Self supporting 0.05 μm Ni foils were used to separate the target gas from the accelerator vacuum system. A liquid nitrogen trap in contact with the target gas was used to minimize contamination. The scattered protons and recoil He^3 particles were detected with silicon surface barrier detectors.

The estimated root-mean-square uncertainty of these cross section measurements due to possible errors in geometry, detection efficiency, current integration, and gas pressure is approximately 3 %. In addition, the statistical uncertainty due to the number of counts was between 2 % and 3 % for centre-of-mass angles between 40° and 100° and was approximately 1 % for all other angles. This order of precision was checked at the beginning of each run by scattering protons from hydrogen; in all cases the observed differential cross sections agreed with the published data to within ± 1 % [13]). It was possible to resolve the protons scattered from heavy impurities at all angles, and any uncertainty arising from this source is included in that for detection efficiency. The energy scale was obtained from the 3.47 MeV resonance in the scattering of protons from O^{16}, giving an estimated precision in the energy of ± 20 keV.

3. Experimental Data

In the scattering of neutrons from He^3 and H^3, broad maxima are observed at 1.9 MeV and 3.5 MeV respectively [14, 15]). This structure is also seen in the scattering

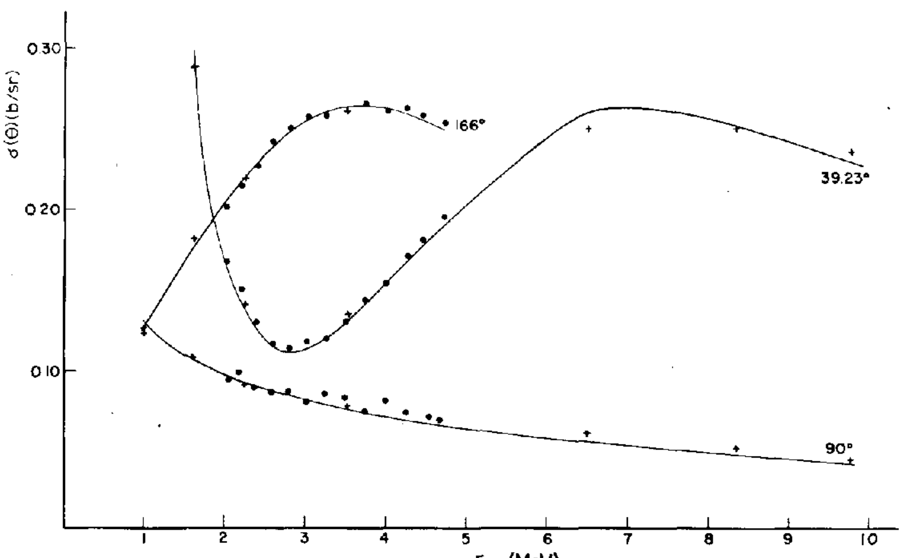

Fig. 1. $He^3(p, p)He^3$ excitation curves corresponding to centre-of-mass angles 39.23°, 90°, and 166°. The energy scale is the proton bombarding energy, and the cross sections are expressed in the centre-of-mass system. The closed circles are the new data; the crosses have been interpolated from previously published work. The smooth curves were calculated from the derived phase shifts.

of protons from He^3. These curves are shown in figs. 1, 2 and 3; the closed circles represent the new data, while the crosses are interpolated from the published data

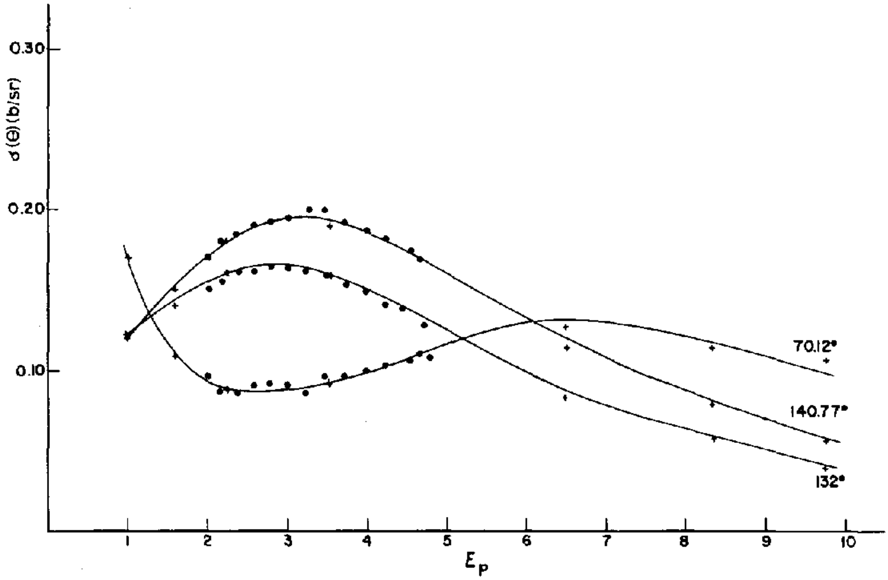

Fig. 2. $He^3(p, p)He^3$ excitation curves corresponding to centre-of-mass angles 70.12°, 132°, and 140.77°. The symbols and curves have the same significance as those defined in fig. 1.

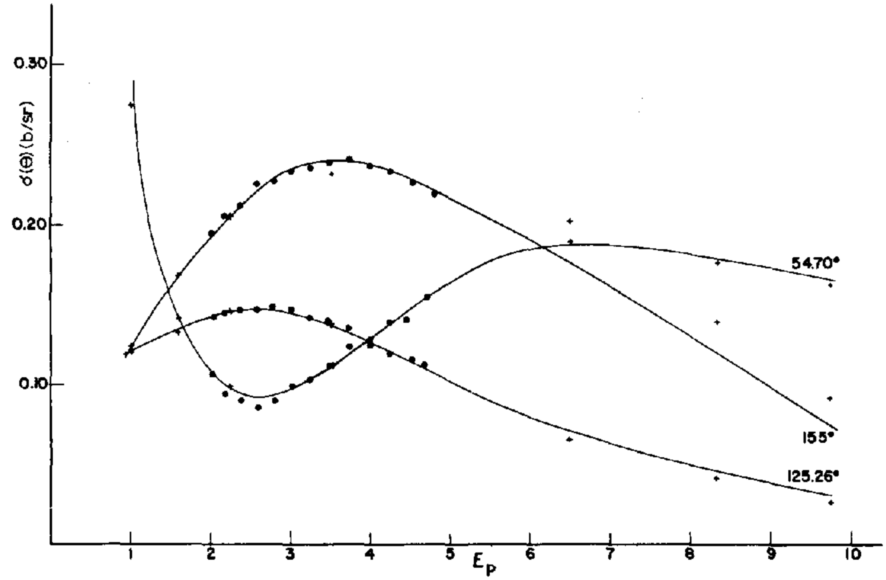

Fig. 3. $He^3(p, p)He^3$ excitation curves corresponding to centre-of-mass angles 54.70°, 125.26°, and 155°. The symbols and curves have the same significance as those defined in fig. 1.

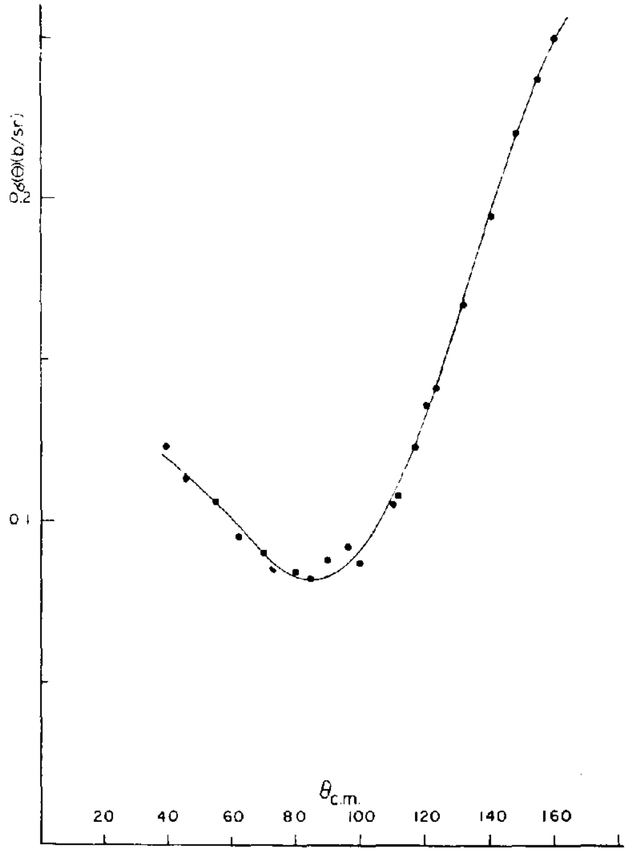

Fig. 4. $He^3(p, p)He^3$ angular distribution at 2.01 MeV bombarding energy. Differential cross sections are given in the centre-of-mass system. The phase shifts used to calculate the solid curve are $\delta_0 = -33.9°$, $\delta_1 = 11.5°$ and $\delta_2 = -0.4°$.

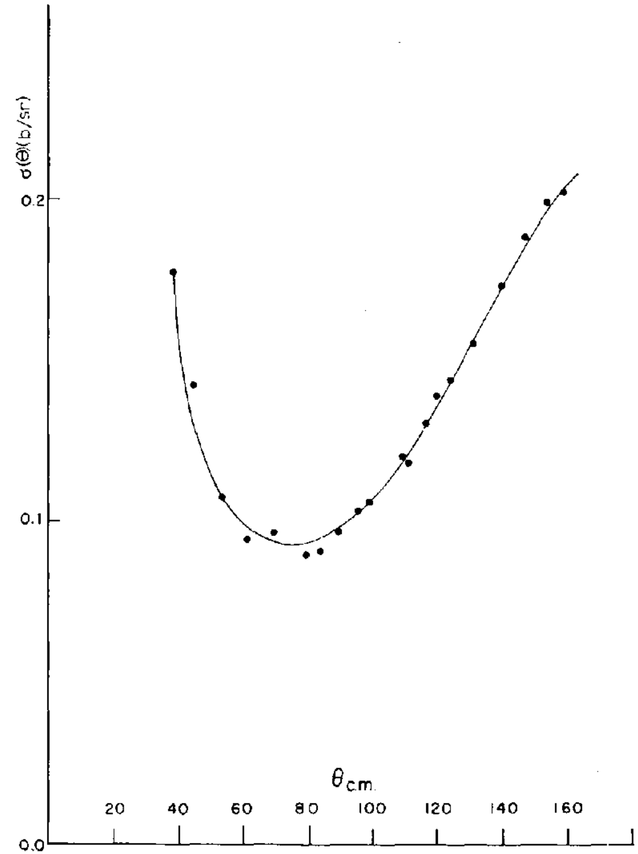

Fig. 5. $He^3(p, p)He^3$ angular distribution at 3.01 MeV bombarding energy. The phase shifts used to calculate the solid curve are $\delta_0 = -45.0°$, $\delta_1 = 22.0°$ and $\delta_2 = -0.6°$.

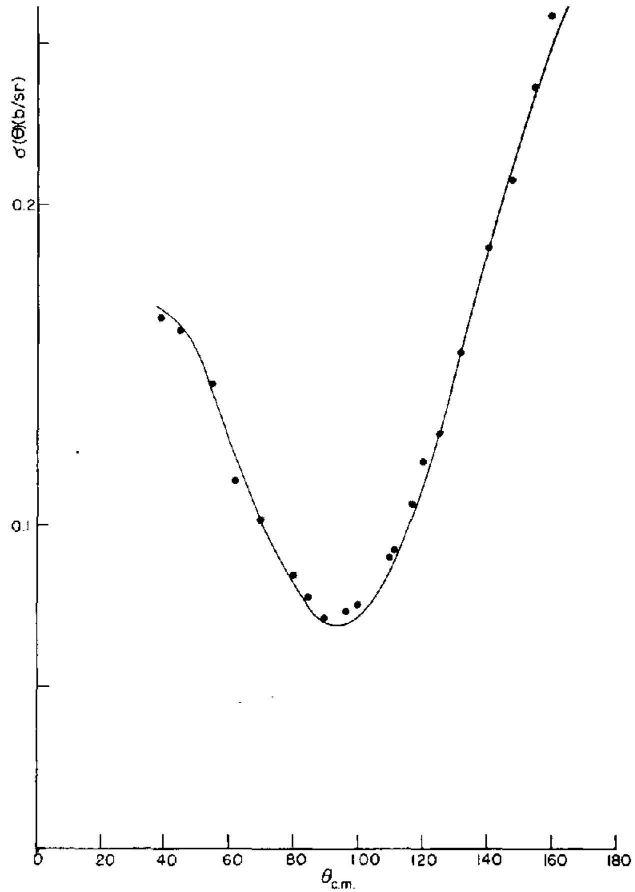

Fig. 6. $He^3(p, p)He^3$ angular distribution at 3.99 MeV bombarding energy. The phase shifts used to calculate the solid curve are $\delta_0 = -51.7°$, $\delta_1 = 31.6°$ and $\delta_2 = -0.5°$.

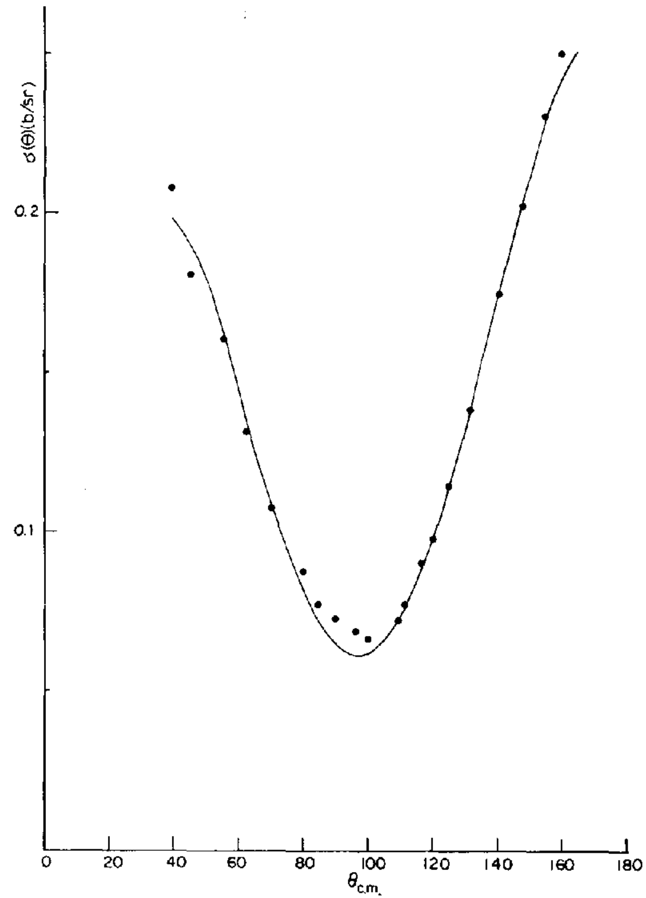

Fig. 7. $He^3(p, p)He^3$ angular distribution at 4.54 MeV bombarding energy. The phase shifts used to calculate the solid curve are $\delta_0 = -55.3°$, $\delta_1 = 35.7°$ and $\delta_2 = -0.8°$.

of Famularo *et al.* [4]), Brolley *et al.* [8]) and Lovberg [6]). The solid lines represent the fit from the phase shift analysis to be discussed in the next section. It is interesting to note that although eight of the excitation curves show pronounced maxima or minima, the cross section at 90° has only a smooth, monotonic decrease with bombarding energy. This, of course, might be interpreted as evidence for a strong P wave interaction, in which there is little splitting of the triplet P wave phase shifts. (Any splitting of these phase shifts would introduce a term with a $\sin^2\theta$ dependence into the differential cross section.)

The angular distributions are shown in figs. 4-7. The solid line represents the fit given by the phase shift analysis.

4. The Phase Shift Analysis

The formula for the differential cross section in the centre-of-mass system is

$$\sigma(\theta) = \frac{1}{2k^2}(|a|^2+|b|^2+|c|^2+|d|^2+|e|^2+|f|^2+|g|^2+|h|^2),$$

where

$$a = \tfrac{1}{2}i\eta \operatorname{cosc}^2 \tfrac{1}{2}\theta e^{i\eta \ln \operatorname{cosc}^2 \frac{1}{2}\theta} + \sum_{l=0}^{\infty} \tfrac{1}{4}P_l(\cos\theta)\{-\sqrt{l(l-1)}U^{l-1}_{(l,1;l-2,1)}$$
$$+(l+2)U^{l+1}_{(l,1;l,1)}+(2l+1)U^{l}_{(l,1;l,1)}+(l-1)U^{l-1}_{(l,1;l,1)}-\sqrt{(l+1)(l+2)}U^{l+1}_{(l,1;l+2,1)}\},$$

$$b = \tfrac{1}{2}i\eta \operatorname{cosc}^2 \tfrac{1}{2}\theta e^{i\eta \ln \operatorname{cosc}^2 \frac{1}{2}\theta} + \sum_{l=0}^{\infty} \tfrac{1}{4}P_l(\cos\theta)\{\sqrt{l(l-1)}U^{l-1}_{(l,1;l-2,1)}+(l+1)U^{l+1}_{(l,1;l,1)}$$
$$+lU^{l-1}_{(l,1;l,1)}+\sqrt{(l+1)(l+2)}U^{l+1}_{(l,1;l+2,1)}+(2l+1)U^{l}_{(l,0,l,0)}\},$$

$$c = \sum_{l=0}^{\infty} \tfrac{1}{4}P_l(\cos\theta)\{\sqrt{l(l-1)}U^{l-1}_{(l,1;l-2,1)}+(l+1)U^{l+1}_{(l,1;l,1)}$$
$$+lU^{l-1}_{(l,1;l,1)}+\sqrt{(l+1)(l+2)}U^{l+1}_{(l,1;l+2,1)}-(2l+1)U^{l}_{(l,0;l,0)}\},$$

$$d = \sum_{l=1}^{\infty} -\tfrac{1}{4}i\sin\theta\,\frac{P'_l(\cos\theta)}{\sqrt{l(l+1)}}\{-\sqrt{(l-1)(l+1)}U^{l-1}_{(l,1;l-2,1)}+\sqrt{l(l+1)}U^{l+1}_{(l,1;l,1)}$$
$$-\sqrt{l(l+1)}U^{l-1}_{(l,1;l,1)}+\sqrt{l(l+2)}U^{l+1}_{(l,1;l+2,1)}-(2l+1)U^{l}_{(l,1;l,0)}\},$$

$$e = \sum_{l=1}^{\infty} -\tfrac{1}{4}i\sin\theta\,\frac{P'_l(\cos\theta)}{\sqrt{l(l+1)}}\{-\sqrt{(l-1)(l+1)}U^{l-1}_{(l,1;l-2,1)}+\sqrt{l(l+1)}U^{l+1}_{(l,1;l,1)}$$
$$-\sqrt{l(l+1)}U^{l-1}_{(l,1;l,1)}+\sqrt{l(l+2)}U^{l+1}_{(l,1;l+2,1)}+(2l+1)U^{l}_{(l,1;l,0)}\},$$

$$f = \sum_{l=2}^{\infty} -\tfrac{1}{4}\sin^2\theta \frac{P_l''(\cos\theta)}{\sqrt{(l-1)l(l+1)(l+2)}} \Big\{ -\sqrt{(l+1)(l+2)}U^{l-1}_{(l,1;l-2,1)} + \sqrt{\frac{l(l-1)(l+2)}{l+1}}\, U^{l+1}_{(l,1;l,1)} - (2l+1)\sqrt{\frac{(l-1)(l+2)}{l(l+1)}}\, U^{l}_{(l,1;l,1)} + \sqrt{\frac{(l-1)(l+1)(l+2)}{l}}\, U^{l-1}_{(l,1;l,1)} - \sqrt{l(l-1)}U^{l+1}_{(l,1;l+2,1)} \Big\},$$

$$g = \sum_{l=1}^{\infty} -\tfrac{1}{4}i\sin\theta \frac{P_l'(\cos\theta)}{\sqrt{l(l+1)}} \Big\{ \sqrt{(l-1)(l+1)}U^{l-1}_{(l,1;l-2,1)} + (l+2)\sqrt{\frac{l}{l+1}}\, U^{l+1}_{(l,1;l,1)} - \frac{(2l+1)}{\sqrt{l(l+1)}}\, U^{l}_{(l,1;l,1)} - (l-1)\sqrt{\frac{l+1}{l}}\, U^{l-1}_{(l,1;l,1)} - \sqrt{l(l+2)}U^{l+1}_{(l,1;l+2,1)} - (2l+1)U^{l}_{(l,0;l,1)} \Big\},$$

$$h = \sum_{l=1}^{\infty} -\tfrac{1}{4}i\sin\theta \frac{P_l'(\cos\theta)}{\sqrt{l(l+1)}} \Big\{ \sqrt{(l-1)(l+1)}U^{l-1}_{(l,1;l-2,1)} + (l+2)\sqrt{\frac{l}{l+1}}\, U^{l+1}_{(l,1;l,1)} - \frac{(2l+1)}{\sqrt{l(l+1)}}\, U^{l}_{(l,1;l,1)} - (l-1)\sqrt{\frac{l+1}{l}}\, U^{l-1}_{(l,1;l,1)} - \sqrt{l(l+2)}U^{l+1}_{(l,1;l+2,1)} + (2l+1)U^{l}_{(l,0;l,1)} \Big\},$$

$$U^{j}_{(l',s';l,s)} = e^{i(\alpha_l+\alpha_{l'})}(\delta_{l,l'}\delta_{s,s'} - S^{j}_{(l',s';l,s)}) = U^{j}_{(l,s;l',s')},$$

where $S^{j}_{(l',s';l,s)}$ is the element of the scattering matrix for total angular momentum j connecting initial orbital angular momentum l' and channel spin s', with their final values l and s. In these formulae

$$\eta = \frac{Z_1 Z_2 e^2}{\hbar v}, \qquad k = \frac{\mu v}{\hbar}, \qquad \alpha_0 = 0, \qquad \alpha_l = \sum_{s=1}^{l} \operatorname{arctg}(\eta/s),$$

where v is the relative velocity of the two particles, and μ is the reduced mass of the system.

This expression for the differential cross section may be obtained from the general expressions that are derived by Blatt and Biedenharn and by Bloch [16, 17]). The signs of the elements which connect different values of the orbital angular momentum have been taken to agree with these references. However, it has been shown [18]) that this phase convention does not lead to the proper time reversal invariance of the scattering matrix, and the signs of all the $U^{j}_{(l,1;l+2,1)}$ and $U^{j}_{(l,1;l-2,1)}$ should be changed.

A phase shift analysis of Famularo's data by Lowen [9]) using a single S wave phase shift and a single P wave phase shift produced a fit to the data that was well within the experimental error. A similar analysis of these data by Frank and Gammel [10]) used four phase shifts, one each for the singlet and triplet channel spins for the S and P waves. As might be expected from Lowen's work, a large number of possible sets of these parameters was obtained. Their assumption that there is no splitting of the triplet phase shifts has found some theoretical justification in the resonating group calculations of Bransden [11]) and is consistent with the small polarizations observed by Cranberg [19]) for scattering of neutrons from H^3 and He^3 at 1.1 MeV and 2.15 MeV.

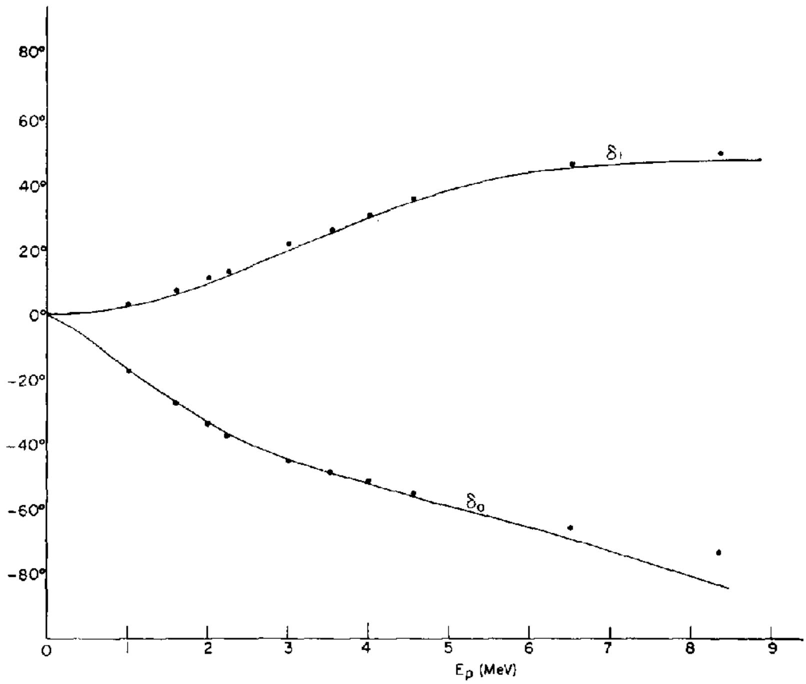

Fig. 8. $He^3(p, p)He^3$ phase shifts, δ_0 and δ_1, in degrees plotted as functions of the bombarding energy. The significance of the solid lines is discussed in the text.

Since it is apparent that a general phase shift analysis would not yield a unique set of parameters, an attempt was made to extend Lowen's analysis to higher energies using a single phase shift for each of the first three partial waves. In this simplified treatment the two S wave phase shifts are set equal, the four P wave shifts are set equal, the four D wave phase shifts are set equal, and all elements which connect either different channel spins or different orbital angular momenta are assumed to vanish. These drastic restrictions simply amount to the assumption that the nuclear interaction of the two particles is completely independent of their spins.

The phase shifts were obtained from the experimental data using the same general procedure that is described in the analysis of the He^4(p, p)He^4 reaction by Miller and Phillips [20]). In addition to the Rice data, the angular distributions of Famularo and of Brolley were also analysed in this way. The S and P wave phase shifts are shown by the closed circles in fig. 8. The D wave phase shift thus obtained was 0.1° at 1.01 MeV and was −1.2° at 8.34 MeV. As is indicated by the angular distributions the fit is quite good at low energies but becomes worse as the energy is increased. It is reasonable to assume that the lack of agreement near 90° reflects the presence of splittings in the triplet phase shifts. A comparison of these phase shifts with the theoretical results of Bransden and Robertson in table 1 indicates that the Serber type of exchange interaction for the nucleon-nucleon potential is favoured over the symmetrical type. This favouring of the Serber type force is in agreement with the results of n-T and n-He^3 scattering in the same energy region [15, 21]). For these reactions, both the shape of the angular distributions and the magnitude of the integrated cross section show much better agreement with the predictions of the Serber interaction then with those of the symmetric interaction.

TABLE 1

The parameters δ_0, δ_1 and δ_2 compared with the theoretical calculations of Bransden and Robertson [11]).

E_p	l	δ_{exp}	δ (Serber)		δ (Symmetrical)	
			$s = 1$	$s = 0$	$s = 1$	$s = 0$
1.00	0	−17.5°	−15.3°	−16.0°	−15.9°	−17.0°
2.50	0	−40.5°	−33.3°	−34.9°	−34.7°	−37.0°
5.00	0	−58.0°	−52.6°	−55.1°	−54.9°	−58.7°
8.00	0	−72.0°	−68.3°	−71.7°	−71.7°	−77.0°
1.00	1	3.7°	3.0°	2.5°	1.9°	1.1°
2.50	1	16.5°	17.9°	13.9°	10.1°	5.5°
5.00	1	39.5°	44.7°	33.8°	25.2°	12.3°
8.00	1	49.0°	55.6°	42.8°	34.0°	15.3°
1.00	2	0.1°	− 0.01°	− 0.02°	− 0.02°	− 0.03°
2.50	2	− 0.5°	− 0.16°	− 0.19°	− 0.21°	− 0.30°
5.00	2	− 0.9°	− 0.71°	− 0.90°	− 1.02°	− 1.48°
8.00	2	− 1.2°	− 1.56°	− 2.04°	− 2.46°	− 3.67°

E_p is the bombarding energy in MeV, and all the phase shifts are given in degrees. The parameter s refers to the channel spin, while the labels "Serber" and "Symmetrical" refer to two of the possible types of exchange interaction for the nucleon-nucleon potential.

The solid lines shown in fig. 8 indicate an attempt to describe these phase shifts in terms of the single-level parameterization. The line fitting δ_0 is that for scattering from a charged, hard-sphere of radius 3.5 fm. The parameters used in fitting δ_1 are $R = 3.5$ fm, E_{Res}(C.M.) $= 26$ MeV, and $\gamma^2 = 22$ MeV. This value of the reduced width corresponds to a ratio to the Wigner limit of 3.2, and thus would tend to preclude the existence of an isolated level, if this oversimplified analysis were taken seriously.

Since in this analysis δ_1 has been taken to represent five P wave parameters, the fact that it increases in a positive sense might indicate that a single one of the P wave phase shifts, corresponding to a particular value of j, has a true resonance character. This possibility was investigated in detail for all the P wave parameters in turn and does not allow a fit to the data to be made over the entire energy range, if reasonable constraints are placed on the non-resonant phase shifts. In addition, there is some indication that a fit is impossible even if one assumes that there are two P wave resonances with different values of j in this energy region.

Though no simple interpretation of these results in terms of nuclear levels is apparent, the positively increasing trend of the P wave parameter tends to show that the presence of such levels cannot be definitely excluded.

We wish to thank R. F. Christy, T. Lauritsen and C. A. Barnes for helpful discussions concerning these results. One of us (T.A.T.) would like to express his appreciation to the staff of the Kellogg Radiation Laboratory for their hospitality and for the use of their Datatron 220 computer.

References

1) I. G. Balashko, I. I. Barit and I. A. Gontcharow, Nuclear forces and the few-nucleon problem (Pergamon Press, New York, 1960) Vol. 2, p. 619
2) N. A. Vlasov, S. P. Kalinin, A. A. Ogloblin, L. N. Samoilov, V. A. Sidorov and V. I. Chuev, JETP **1** (1955) 500
3) A. I. Baz' and Ia. A. Smorodinskii, JETP **27** (1954) 382
4) K. F. Famularo, R. J. S. Brown, H. D. Holmgren and T. F. Stratton, Phys. Rev. **93** (1954) 928
5) D. R. Sweetman, Phil. Mag. **46** (1955) 358
6) R. H. Lovberg, Phys. Rev. **103** (1956) 1393
7) K. P. Artemov, S. P. Kalinin and L. N. Samilov, JETP **10** (1959) 474
8) J. E. Brolley, Jr., T. M. Putnam, L. Rosen and L. Stewart, Phys. Rev. **117** (1960) 1307
9) R. W. Lowen, Phys. Rev. **96** (1954) 826
10) R. M. Frank and J. L. Gammel, Phys. Rev. **99** (1955) 1406
11) B. H. Bransden, H. H. Robertson and P. Swan, Proc. Phys. Soc. **A69** (1956) 877; B. H. Bransden and H. H. Robertson, Proc. Phys. Soc. **A72** (1958) 770
12) C. Miller Jones, G. C. Phillips, R. W. Harris and E. H. Beckner, Nuclear Physics **37** (1962) 1
13) D. J. Knecht, S. Messelt, E. D. Berners and L. C. Northcliffe, Phys. Rev. **114** (1959) 550
14) Los Alamos Physics and Cryogenics Groups, Nuclear Physics **12** (1959) 299
15) A. R. Sayres, K. W. Jones and C. S. Wu, Phys. Rev. **122** (1961) 1853
16) J. Blatt and L. C. Biedenharn, Rev. Mod. Phys. **24** (1952) 258
17) C. Bloch, La théorie des réactions nucléaires (Commissariat à l'Energie Atomique, Service de Documentation, Saclay, 1955)
18) A. M. Baldin, V. I. Gol'danskii and I. L. Rozenthal, Kinematics of nuclear reactions (Pergamon Press, New York, 1964) p. 168
19) L. Cranberg, Nuclear forces and the few-nucleon problem (Pergamon Press, New York, 1960) Vol. 2, p. 473
20) P. D. Miller and G. C. Phillips, Phys. Rev. **112** (1958) 2043
21) J. D. Seagrave, L. Cranberg and J. E. Simmons, Phys. Rev. **119** (1960) 1981